



## The Comparison of Neutron Beams through ${}^7\text{Li}(p,n)$ Reactions for the Design of a Thermal Neutron Radiography Facility using the MCNPX Code

J. G. Fantidis<sup>\*a</sup>, G. E. Nicolaou<sup>b</sup>

<sup>a</sup> Department of Electrical Engineering-Department of Physics, International Hellenic University, Kavala, Greece

<sup>b</sup> Laboratory of Nuclear Technology, School of Engineering, 'Democritus' University of Thrace, Xanthi, Greece

### PAPER INFO

#### Paper history:

Received 10 May 2020

Received in revised form 13 June 2020

Accepted 03 September 2020

#### Keywords:

${}^7\text{Li}(p,n)$  Reaction

MCNPX Monte Carlo Code

Non Destructive Testing

Thermal Neutron Radiography

### ABSTRACT

In this work, a comparison of six neutron beams was carried out using the MCNPX Monte Carlo code for thermal neutron radiography purposes. The necessary neutrons produced via the  ${}^7\text{Li}(p,n)$  reaction for 1 mA proton beam with energies 2.3, 2.5, 3, 4, 4.5, and 5 MeV. The design of the facility was governed from the purpose to achieve the maximum thermal neutron flux in the position of the investigated object. An extensive number of simulations were realized for every source under different conditions. The higher energy of proton beam provides higher intensity for the neutron source but at the same time, the produced spectrum shifted to the fast neutron area. Protons with energies from 2.3 to 3 MeV are more suitable when the thermal neutron content is the main issue of the facility design. Neutrons produced by proton beam in the energy range of 4–5 MeV provide higher thermal neutron fluxes at the cost of the thermal neutron content. The final choice is a compromise, between the thermal neutron content that can be tolerated, in combination with a workable thermal neutron flux.

doi: 10.5829/ije.2020.33.11b.12

## 1. INTRODUCTION

Radiography without a doubt is the most widespread non-destructive testing (NDT) in human history. Radiography today uses not only gamma or X-rays but also electrons, protons, and neutrons. Neutron radiography (NR) is maybe the most interesting case because neutron seems to be a complementary method compared to the powerful and most commonly used X-ray imaging. X-rays (and gamma rays) can penetrate effortlessly through light materials but cannot pass dense materials. Neutrons on the contrary direction easily penetrate even the dense metals, conversely attenuate strongly through some light elements such as hydrogen, boron, or lithium. The thermal neutrons range is the most interest for NR because in this range the neutrons have higher cross-sections and their detection is more efficient. Compared to the X-ray radiography thermal NR facilities are rather rare. The reason for this is the lack of high-intensity sources [1–3].

According to many previous works to increase not only the thermal NR units but also many other facilities, there is a need for non-reactor high-intensity neutron sources [3–6]. Accelerators although are not "low-priced" but have a considerably lower cost than nuclear reactors or spallation neutron sources, and seem like the most suitable solution. Proton, electrons, deuterium, and tritium accelerators on heavy or light materials target have been proposed; however, based on the results the  ${}^7\text{Li}(p,n)$  reaction is the best solution both for thermal and epithermal neutrons beams because offer both soft spectrum and high-intensity neutron yield. Neutrons via  ${}^7\text{Li}(p,n)$  reaction can be used for thermal NR, for Boron Neutron Capture Therapy, for medical isotope production, for physics cross-section experiments, and for the development of a quasi monoenergetic neutron beam [7–9].

However, the  ${}^7\text{Li}(p,n)$  reaction requires special attention because the lithium metal has poor mechanical and chemical properties. In addition, based on the fact

\*Corresponding Author Institutional Email: [fantidis@teiemt.gr](mailto:fantidis@teiemt.gr)  
(J. G. Fantidis)

that has a rather low melting temperature ( $\approx 180^\circ\text{C}$ ) is necessary for the presence of an appropriate cooling system. Previous works from Bayanov et al. have indicated that is possible to cool a lithium target with water using up to 10mA proton beam [10, 11]. The energy of the protons determines the total neutron yield, the maximum and the minimum energy of the emitted neutrons. The increment of the energy in the protons beam increases the neutron flux but simultaneously provides a harder spectrum so a compromise is necessary.

A representative unit for thermal NR based on Deuterium-Tritium, Deuterium-Deuterium or Tritium-Tritium neutron generators,  $^{252}\text{Cf}$ ,  $^{241}\text{Am/Be}$  isotopic neutron sources, and proton or electron accelerators usually on beryllium target [3, 7, 12–14]. The use of proton accelerators in a lithium target for NR facilities is rare. In this article, the proposed thermal NR facility improves the only previous similar proposed system [9] in four ways. Firstly, by using 6 different proton beam energy; secondly, to maximize the thermal neutron flux in the object the angle between the proton beam and the collimator was  $0^\circ$ ; thirdly, by using a smaller disk source with a lower proton beam current which reduces considerably the scattered neutrons and fourthly, optimizing the divergent collimator dimensions. Hence, this work aims to evaluate the performance of a thermal NR facility based on neutrons emitted when the lithium target bombarded by protons beams with 6 different energies 2.3, 2.5, 3, 4, 4.5, and 5 MeV. The facility firstly modified to maximize the flux of the thermal neutrons and secondly the quality of the beam enhanced using a sapphire filter. Both the design and the calculations have been simulated with the help of the MCNPX 2.5.0 Monte Carlo code [15, 16]. For this article, the results are based on the use of 1 mA protons beams as a result the presented facility does not require any special cooling system for the lithium target [7].

## 2. MATERIAL AND METHODS

**2. 1. Neutron Source** Although there are many articles that study and measure the neutron yield from lithium target for different energy of proton accelerator some discrepancies still exist [17, 18]. Theoretical the neutron yield emitted per second into solid angle  $d\Omega$  when a thick lithium target bombarded by a proton beam can be calculated from the equation [19, 20]:

$$\frac{d^2N}{d\Omega dE_n} = i g D \left( \frac{d\sigma_{pn}}{d\Omega} \right)_{\text{CMS}} \frac{d\Omega_{\text{CMS}}}{d\Omega} \frac{dE_p}{dE_n} S^{-1}(E_p) \quad (1)$$

where  $i$  is the proton beam current in  $\mu\text{A}$ ,  $g$  gives the number of protons per  $\mu\text{A}$ ,  $D$  is the atomic density of  $^7\text{Li}$ ,  $\left( \frac{d\sigma_{pn}}{d\Omega} \right)_{\text{CMS}}$  describes the differential cross-section for the  $^7\text{Li}(p,n)$  reaction,  $E_p$  is the proton energy,  $E_n$  is the energy

of the emitted neutrons in the solid angle  $\Omega$  and  $S^{-1}(E_p)$  is the inverse stopping power in lithium.

In this article 6 protons beams with energies 2.3, 2.5, 3, 4, 4.5, and 5 MeV bombard thick lithium target. The lithium target is a disk with 4 cm diameter and  $100\mu\text{m}$  thickness with the intention to minimize the unwanted flux of 478 keV  $\gamma$ -rays [15, 16]. The spectra of the emitted neutrons are shown in Figure 1 for proton current equal to 1 mA. The estimated total neutron yields are  $5.78 \times 10^{11}$ ,  $8.83 \times 10^{11}$ ,  $1.56 \times 10^{12}$ ,  $3.62 \times 10^{12}$ ,  $4.96 \times 10^{12}$ , and  $6.48 \times 10^{12}$   $\text{ncm}^{-2}\text{s}^{-1}$  for 2.3, 2.5, 3, 4, 4.5, and 5 MeV protons beams respectively. From the spectra is obvious that despite the relatively soft spectra more thermalization of the beams is necessary. According to many previous works, the best material for this purpose is the high-density polyethylene (HD-PE) so HD-PE was selected as a neutron moderator [3, 12].

**2. 2. Collimator Design** There are a number of parameters that govern the quality of the radiography produced by a thermal NR facility. The most important parameter is the L/D ratio, where L is the length of the collimator and D is the diameter of the inlet aperture. L/D ratio is used as an indicator of the efficacy of the neutron beam. A large L/D ratio value means better spatial resolution but in the same time decreases the thermal neutron flux ( $f_{\text{th}}$ ) in the investigated object so is necessary a mutual compromise between high spatial resolution and high  $f_{\text{th}}$ . The part of neutrons lost due to collimation defining by the ratio [2]:

$$\varphi_i = 16 \cdot \varphi_o \left( \frac{L}{D} \right)^2 \quad (2)$$

where  $\varphi_i$  describes neutron intensity at the entrance to the collimator and  $\varphi_o$  is neutron flux at the exit of the collimator. The spatial resolution losses can be calculated by the geometric unsharpness  $u_g$  [2]:

$$u_g = L_f \cdot \left( \frac{D}{L_s} \right) \quad (3)$$

where  $L_s$  expresses the neutron source to investigated object distance and  $L_f$  is the image to object distance (usual equal to 0.5 cm). The divergence of the neutron beam is described by the equation [2]:

$$\theta = \tan^{-1} \left( \frac{I}{2L} \right) \quad (4)$$

where  $\theta$  gives the half-angle of the beam divergence,  $I$  is the maximum dimension of the image plane and  $L$  is the length of the divergent collimator. Thermal neutron content (TNC) is the number of thermal neutrons within the neutron beam. Usually, this parameter has small values which can be improved using fast neutrons filters. The  $n/\gamma$  ratio, which is the ratio of neutron intensity of the beam versus the gamma components, is a factor that creates noise in the radiographic image and has suggested value  $> 10^4$   $\text{ncm}^{-2}\text{mSv}^{-1}$  [1, 2].

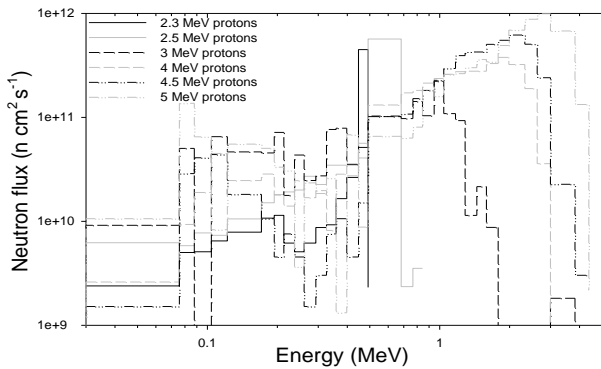


Figure 1. Neutron spectra for 1mA proton current

### 2. 3. Thermal Neutron Radiography Facility

The geometrical configuration of the proposed facility is shown in Figure 2. All the presented dimensions have been chosen with a criterion to provide the maximum  $f_{th}$ . Next to the neutron source, there is HD-PE moderator, the parameter  $a$  (distance between the source and convergent collimator) is equal to 1.4 cm for the 2.3 MeV proton beam and 1.7 cm for the others beams. The divergent collimator has a conical shape with radii 1.5 and 1 cm with the bigger one on the side of the source. The length  $b$  of the divergent collimator is 10 cm for the 2.3 and 2.5 MeV proton beams, 11 cm for 3, 4, 4.5 MeV proton beams, and 12 cm for the 5 MeV proton beam. The divergent collimator is void but to improve the TNC parameter can be filled with a single sapphire filter which is an excellent fast neutron filter [21].

Next to the convergent collimator, there is a divergent collimator with variable length ( $L = 50-200$  cm) while the inlet aperture ( $D$ ) is 1 cm. The divergent collimator has as lining material Boral with thickness 0.8 cm, while borated polyethylene (PE-B) and bismuth (bi) with thicknesses 3.2 and 1 cm were selected as filling materials. The aperture in the side of the investigated object ( $D_0$ ) has a changeable dimension (14–18 cm). Boral and bi were also chosen as materials for the configuration of the aperture with dimensions 0.8 and 1.2 cm correspondingly; the first prevents the stray and scattered neutrons and the second minimizes the unwanted gamma-rays.

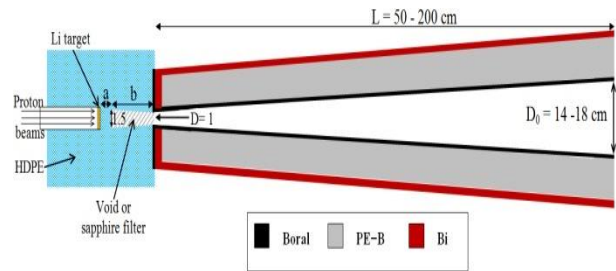


Figure 2. Geometric configuration of the simulated facility

### 3. RESULTS AND DISCUSSION

To evaluate and compare the 6 beams the presented facility was simulated for a wide range of the parameters which characterize a thermal NR unit.  $L/D$  ratio has values from 50 to 200, divergence angle ( $\theta$ ) varies from  $1.29-4^\circ$  and the geometric unsharpness diversifies from  $2.5 \times 10^{-3}$  up to  $1 \times 10^{-2}$ . In this work, the  $n/\gamma$  ratio values are not presented because in each simulation has a value of at least two orders of magnitude higher than the recommended value ( $10^4$  n-cm $^{-2}$ -mSv $^{-1}$ ). The  $f_{th}$  (with energy 0.01–0.3 eV) was calculated with the MCNPX code using the surface tally (F2). F2 tally calculates the averaged neutron flux in a surface in neutrons cm $^{-2}$  per starting neutron. In the presented facility this surface was placed 0.5 cm away from the divergent collimator and has a radius equal to the aperture beside the image detector [2].

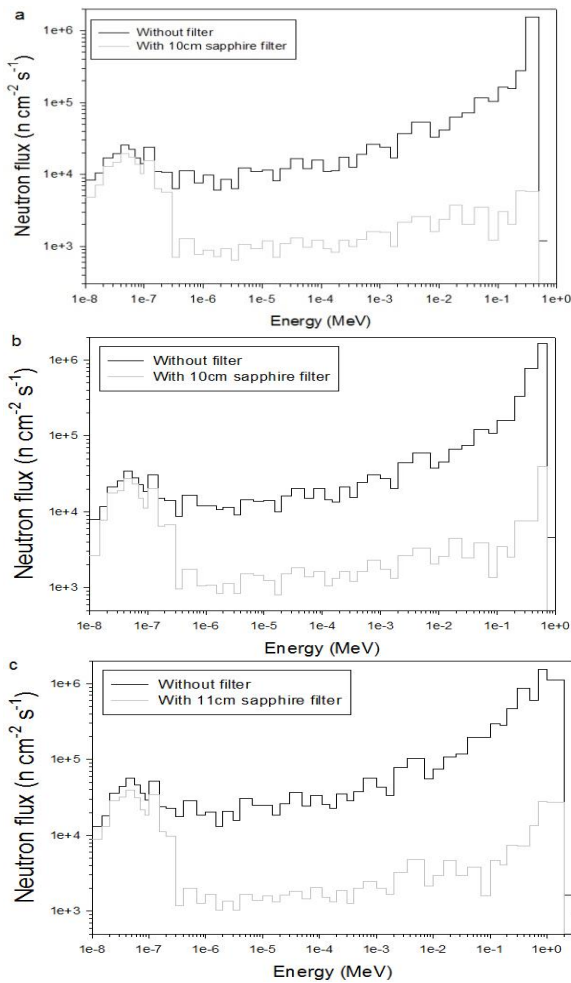
$f_{th}$  and TNC parameters for every source and for the different values of the basic parameters are shown in Table 1. From these results, it is evident that the 2.3 MeV proton beam offers the higher values for the TNC parameter but the minimum  $f_{th}$  in each simulation. In the opposite direction, the 5 MeV proton beam owing to the higher neutron yield provides the higher intensities for the  $f_{th}$  but with the smaller TNC values. For the same configurations, the  $f_{th}$  varies by a factor up to 5.43, in the same conditions the TNC fluctuates by a factor up to 2.27. However, in every simulation, the TNC has values less than 5.9%, which is not always practical. To overcome this drawback, the use of a fast neutron filter is necessary. Figures 3a-3c show the beam profile at the image plane with and without a single sapphire filter in

TABLE 1. Thermal NR calculated parameters for the 6 beams and for different L/D values

L/D	L (cm)	D0 (cm)	$\theta$ (deg)	$U_g$ (cm)	2.3 MeV proton		2.5 MeV proton		3 MeV proton		4 MeV proton		4.5 MeV proton		5 MeV proton	
					$f_{th}$ (ncm $^{-2}$ s $^{-1}$ )	TNC (%)	$f_{th}$ (ncm $^{-2}$ s $^{-1}$ )	TNC (%)	$f_{th}$ (ncm $^{-2}$ s $^{-1}$ )	TNC (%)	$f_{th}$ (ncm $^{-2}$ s $^{-1}$ )	TNC (%)	$f_{th}$ (ncm $^{-2}$ s $^{-1}$ )	TNC (%)	$f_{th}$ (ncm $^{-2}$ s $^{-1}$ )	TNC (%)
50	50	14	4.00	1.00E-2	1.82E+5	5.85	2.29E+5	5.47	3.75E+5	5.25	5.98E+5	3.04	7.54E+5	2.77	9.69E+5	2.72
100	100	16	2.29	5.00E-3	4.67E+4	5.55	6.11E+4	5.40	9.95E+4	5.12	1.43E+5	2.69	1.86E+5	2.52	2.38E+5	2.45
150	150	18	1.71	3.33E-3	2.05E+4	5.37	2.66E+4	5.17	4.44E+4	5.02	6.54E+4	2.69	8.18E+4	2.43	1.08E+5	2.43
200	200	18	1.29	2.50 E-3	1.14E+4	5.29	1.47E+4	5.04	2.59E+4	5.01	3.75E+4	2.70	4.69E+4	2.44	6.08E+4	2.40

the convergent collimator for  $L/D = 50$ . The thermal neutrons (0.01–0.3 eV) are separated in 10 groups, the epithermal neutrons energy range (0.3 eV–0.1 Mev) are arranged in 26 groups and the fast neutrons are divided in 11 bands. The presence of the filter reduces significantly the fast neutrons in the cases of 2.3, 2.5, and 3 MeV protons beams, without important consequence on the thermal neutrons energy range.

Figures 4a-4c illustrate that for harder neutron spectra although there is a noticeable reduction in the fast neutrons band the quantity of them is still rather high. The thermal energy range presents again a small decrement.  $f_{th}$  and TNC parameters were also calculated for each source and each  $L/D$  ratio for 3 different thickness of the sapphire filter. For the 2.3 MeV proton beam, the results are listed in Table 2. The TNC parameter is nearly stable for the same thickness of the sapphire filter and practical independent of the  $L/D$  ratio. The TNC is about 18%, 37%, and 68% for 3, 6 and 10, cm thicknesses of the



**Figure 3.** Neutron spectra at the image position for  $L/D=50$ , a) 2.3 MeV, b) 2.5 MeV, c) 3 MeV protons energy respectively

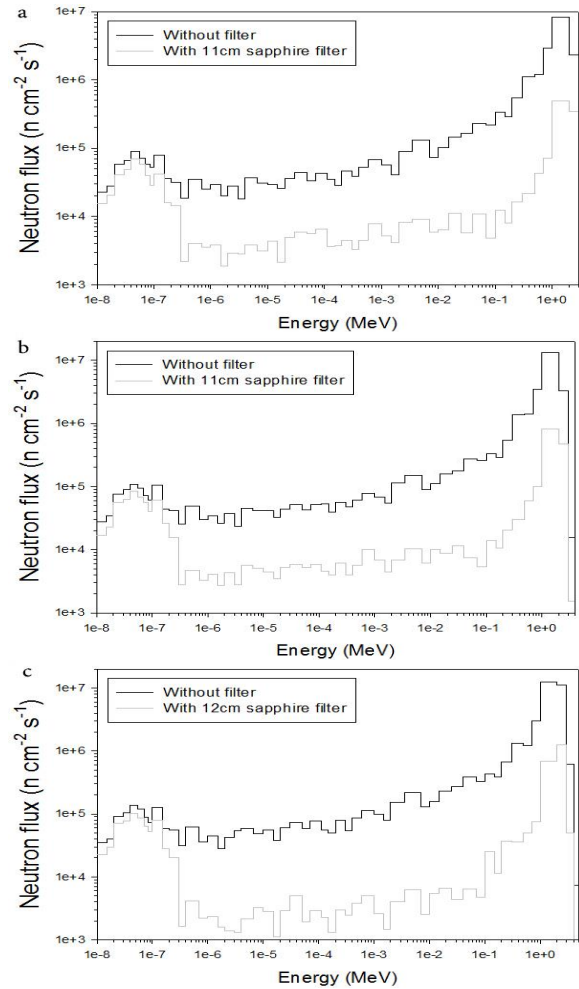


**Figure 4.** Neutron spectra at the image position for  $L/D=50$ , a) 4 MeV, b) 4.5 MeV, c) 5 MeV protons energy respectively

filter respectively. At the same time, the reduction of the  $f_{th}$  is about 11%, 21%, and 33%. The second beam gives lower TNC values for the same thicknesses of the filter with percentages in the region of 13%, 28%, and 57% and a similar tendency for the  $f_{th}$  (Table 3). Similar

**TABLE 2.** Thermal NR simulated parameters using a proton beam with energy 2.3 MeV

L/D	Sapphire filter (cm)					
	3		6		10	
	$f_{th}$ ( $ncm^{-2}s^{-1}$ )	TNC (%)	$f_{th}$ ( $ncm^{-2}s^{-1}$ )	TNC (%)	$f_{th}$ ( $ncm^{-2}s^{-1}$ )	TNC (%)
50	2.49E+5	18.55	2.21E+5	37.85	1.93E+5	67.90
100	6.38E+4	18.34	5.67E+4	37.36	4.95E+4	68.27
150	2.80E+4	17.94	2.48E+4	37.17	2.17E+4	67.97
200	1.56E+4	17.80	1.39E+4	36.88	1.21E+4	67.62

**TABLE 3.** Thermal NR simulated parameters using a proton beam with energy 2.5 MeV

L/D	Sapphire filter (cm)					
	3		6		10	
	$f_{th}$ ( $ncm^{-2}s^{-1}$ )	TNC (%)	$f_{th}$ ( $ncm^{-2}s^{-1}$ )	TNC (%)	$f_{th}$ ( $ncm^{-2}s^{-1}$ )	TNC (%)
50	2.05E+5	13.40	1.82E+5	28.90	1.59E+5	58.13
100	5.46E+4	13.43	4.86E+4	29.26	4.24E+4	58.35
150	2.38E+4	12.95	2.12E+4	28.55	1.85E+4	58.37
200	1.32E+4	12.70	1.17E+4	28.07	1.02E+4	57.95

behavior, both for the TNC and the  $f_{th}$ , presents and the 3 MeV proton beam. The filter with thickness 3, 6, and 11 cm reduces the  $f_{th}$  by a factor 1.12, 1.26, and 1.48 respectively, at the same time the TNC ratio is about 12%, 28%, and 64% (Table 4).

For proton energy  $> 3$  MeV the neutron spectra are harder so the TNC parameter gives lower percentages while the  $f_{th}$  does not have significant alteration, with a decrement in the flux similar to the previous cases. Table 5 shows the results for the 4 MeV proton beam for 3, 6, and 11 cm of a sapphire filter; the TNC is approximately 5%, 11%, and 27% correspondingly. In the case of 4.5 MeV proton beam (Table 6) for the same thicknesses of the filter, the TNC values are lower compared with the 4

**TABLE 4.** Thermal NR simulated parameters using a proton beam with energy 3 MeV

L/D	Sapphire filter (cm)					
	3		6		11	
	$f_{th}$ ( $ncm^{-2}s^{-1}$ )	TNC (%)	$f_{th}$ ( $ncm^{-2}s^{-1}$ )	TNC (%)	$f_{th}$ ( $ncm^{-2}s^{-1}$ )	TNC (%)
50	3.36E+5	13.06	2.99E+5	27.87	2.54E+5	61.77
100	8.90E+4	12.94	7.91E+4	28.03	6.73E+4	64.19
150	3.97E+4	12.81	3.53E+4	27.99	3.00E+4	64.17
200	2.32E+4	13.14	2.06E+4	28.80	1.75E+4	65.66

**TABLE 5.** Thermal NR simulated parameters using a proton beam with energy 4 MeV

L/D	Sapphire filter (cm)					
	3		6		11	
	$f_{th}$ ( $ncm^{-2}s^{-1}$ )	TNC (%)	$f_{th}$ ( $ncm^{-2}s^{-1}$ )	TNC (%)	$f_{th}$ ( $ncm^{-2}s^{-1}$ )	TNC (%)
50	5.35E+5	6.37	4.75E+5	12.09	4.04E+5	25.76
100	1.28E+5	5.77	1.14E+5	11.48	9.65E+4	27.18
150	5.85E+4	5.00	5.20E+4	11.68	4.42E+4	28.83
200	3.36E+4	5.87	2.98E+4	11.91	2.54E+4	29.98

MeV proton beam (5%, 10%, and 25%). As expected the neutrons produced by 5 MeV proton beam provide the lower TNC values owing to the harder spectra so the TNC for 3, 6, and 12 cm of sapphire filter has values about 5%, 9%, and 21% respectively (Table 7).

**TABLE 6.** Thermal NR simulated parameters using a proton beam with energy 4.5 MeV

L/D	Sapphire filter (cm)					
	3		6		11	
	$f_{th}$ ( $ncm^{-2}s^{-1}$ )	TNC (%)	$f_{th}$ ( $ncm^{-2}s^{-1}$ )	TNC (%)	$f_{th}$ ( $ncm^{-2}s^{-1}$ )	TNC (%)
50	6.74E+5	5.76	5.99E+5	10.90	5.10E+5	23.13
100	1.67E+5	5.34	1.48E+5	10.55	1.26E+5	24.92
150	7.31E+4	5.12	6.50E+4	10.16	5.53E+4	25.76
200	4.19E+4	5.20	3.72E+4	10.45	3.17E+4	26.73

**TABLE 7.** Thermal NR simulated parameters using a proton beam with energy 5 MeV

L/D	Sapphire filter (cm)					
	3		6		12	
	$f_{th}$ ( $ncm^{-2}s^{-1}$ )	TNC (%)	$f_{th}$ ( $ncm^{-2}s^{-1}$ )	TNC (%)	$f_{th}$ ( $ncm^{-2}s^{-1}$ )	TNC (%)
50	8.67E+5	5.10	7.70E+5	9.09	6.33E+5	21.42
100	2.13E+5	4.69	1.89E+5	8.49	1.56E+5	21.49
150	9.68E+4	4.68	8.61E+4	8.52	7.07E+4	22.00
200	5.44E+4	4.63	4.84E+4	8.52	3.97E+4	22.62

#### 4. CONCLUSION

The performance of six neutrons beams generated by  ${}^7\text{Li}(p,n)$  reaction with proton energy in the range between 2.3 up to 5 MeV for a thermal neutron radiography facility was evaluated using the MCNPX Monte Carlo code. The geometrical configuration of the facility has been designed with the intention to maximize the  $f_{th}$  which reaches at the image position. For each source, the facility has been simulated for a wide range of the parameters which characterize every thermal radiography system. To reduce the intensity of the fast neutrons and enhance the quality of the beam a single sapphire was used as a fast neutron filter. The presence of the filter improves drastically the TNC without significant sacrifice in the  $f_{th}$  values. Neutrons which produced by proton energy from 2.3 to 3 MeV provide softer spectra and better TNC values but with lower  $f_{th}$ , on the contrary, neutrons generated by proton energy in the range 4 to 5 MeV offer higher  $f_{th}$  but the TNC, even though the use of a filter, has a relatively low percentage.

For this reason, is compulsory a mutual compromise between  $f_{th}$  and TNC.

## 5. REFERENCES

- Hawkesworth, M. R. "Neutron radiography. Equipment and methods." *Atomic Energy Review*, Vol. 15, No. 2, (1977), 169–220. Retrieved from [http://inis.iaea.org/Search/search.aspx?orig\\_q=RN:8343576](http://inis.iaea.org/Search/search.aspx?orig_q=RN:8343576)
- Hardt, P. von der, and Röttger, H. Neutron radiography handbook: nuclear science and technology. Springer Science & Business Media, 2012.
- Fantidis, J. G. "The use of electron linac for high quality thermal neutron radiography unit." *Nuclear Instruments and Methods in Physics Research, Section A: Accelerators, Spectrometers, Detectors and Associated Equipment*, Vol. 908, (2018), 361–366. <https://doi.org/10.1016/j.nima.2018.08.114>
- Pirouz, F., Najafpour, G., Jahanshahi, M., and Sharifzadeh Baei, M. "Plant-based calcium fructoborate as boron-carrying nanoparticles for neutron cancer therapy." *International Journal of Engineering, Transactions A: Basics*, Vol. 32, No. 4, (2019), 460–466. <https://doi.org/10.5829/ije.2019.32.04a.01>
- Chichester, D. L., Simpson, J. D., and Lemchak, M. "Advanced compact accelerator neutron generator technology for active neutron interrogation field work." *Journal of Radioanalytical and Nuclear Chemistry*, Vol. 271, No. 3, (2007), 629–637. <https://doi.org/10.1007/s10967-007-0318-7>
- Anderson, I. S., Andreani, C., Carpenter, J. M., Festa, G., Gorini, G., Loong, C. K., and Senesi, R. "Research opportunities with compact accelerator-driven neutron sources." *Physics Reports*. Elsevier B.V. <https://doi.org/10.1016/j.physrep.2016.07.007>
- Fantidis, J. G. "A study of a transportable thermal neutron radiography unit based on a compact RFI linac." *Journal of Radioanalytical and Nuclear Chemistry*, Vol. 293, No. 1, (2012), 95–101. <https://doi.org/10.1007/s10967-012-1736-8>
- Mashnik, S. G., Chadwick, M. B., Hughes, H. G., Little, R. C., MacFarlane, R. E., Waters, L. S., and Young, P. G. "7-Li(p,n) Nuclear Data Library for Incident Proton Energies to 150 MeV." In *Proceeding 2000 ANS/ENS International Meeting, Nuclear Applications of Accelerator Technology* (pp. 1–11). Retrieved from <http://arxiv.org/abs/nucl-th/0011066>
- Fantidis, J. G. "Beam shaping assembly study for BNCT facility based on a 2.5 MeV proton accelerator on Li target." *Journal of Theoretical and Applied Physics*, Vol. 12, No. 4, (2018), 249–256. <https://doi.org/10.1007/s40094-018-0312-1>
- Bayanov, B., Belov, V., Kindyuk, V., Oparin, E., and Taskaev, S. "Lithium neutron producing target for BINP accelerator-based neutron source." *Applied Radiation and Isotopes*, Vol. 61, No. 5, (2004), 817–821. <https://doi.org/10.1016/j.apradiso.2004.05.032>
- Bayanov, B., Kashaeva, E., Makarov, A., Malyshkin, G., Samarin, S., and Taskaev, S. "A neutron producing target for BINP accelerator-based neutron source." *Applied Radiation and Isotopes*, Vol. 67, No. 7-8 SUPPL., (2009), S282–S284. <https://doi.org/10.1016/j.apradiso.2009.03.076>
- Da Silva, A. X., and Crispim, V. R. "Study of a neutron radiography system using 252Cf neutron source." *Radiation Physics and Chemistry*, Vol. 61, No. 3, (2001), 515–517. [https://doi.org/10.1016/S0969-806X\(01\)00318-8](https://doi.org/10.1016/S0969-806X(01)00318-8)
- Fantidis, J. G., Nicolaou, G. E., and Tsagas, N. F. "A transportable neutron radiography system." *Journal of Radioanalytical and Nuclear Chemistry*, Vol. 284, No. 2, (2010), 479–484. <https://doi.org/10.1007/s10967-010-0502-z>
- Fantidis, J. G., Bandekas, D. V., Constantinou, P., and Vordos, N. "Fast and thermal neutron radiographies based on a compact neutron generator." *Journal of Theoretical and Applied Physics*, Vol. 6, No. 1, (2012), 1–8. <https://doi.org/10.1186/2251-7235-6-20>
- Hendricks, J. S., Mckinney, G. W., Waters, L. S., Roberts, T. L., Egdorf, H. W., Finch, J. P., Trelle, H. R., Pitcher, E. J., Mayo, D. R., Swinhoe, M. T., Lebenhaft, J. MCNPX extensions version 2.5. 0 (Report No. LA-UR-05-2675), 2005. Retrieved from [https://mcnp.lanl.gov/pdf\\_files/la-ur-05-2675.pdf](https://mcnp.lanl.gov/pdf_files/la-ur-05-2675.pdf)
- Miresghhi, M. "Simulation of a Neutron Detector for Real Time Imaging Applications." *International Journal of Engineering*, Vol. 11, No. 4, (1998), 207–212. Retrieved from [http://www.ije.ir/article\\_71214.html](http://www.ije.ir/article_71214.html)
- Atanackovic, J., Matysiak, W., Witharana, S., Dubeau, J., and Waker, A. J. "Measurements of neutron energy spectra from  ${}^7\text{Li}(p,n){}^7\text{Be}$  reaction with bonner sphere spectrometer, nested Neutron spectrometer and ROSPEC." *Radiation Protection Dosimetry*, Vol. 161, No. 1-4, (2014), 221–224. <https://doi.org/10.1093/rpd/nct314>
- Bakshi, A. K., Dawn, S., Suryanarayana, S. V., and Datta, D. "Spectrometry and dosimetry of neutron beams produced by  ${}^7\text{Li}(p,n)$  reactions in the proton energy range of 3–5 MeV." *Nuclear Instruments and Methods in Physics Research, Section A: Accelerators, Spectrometers, Detectors and Associated Equipment*, Vol. 949, (2020), 162926. <https://doi.org/10.1016/j.nima.2019.162926>
- Allen, D. A., and Beynon, T. D. "A design study for an accelerator-based epithermal neutron beam for BNCT." *Physics in Medicine and Biology*, Vol. 40, No. 5, (1995), 807–821. <https://doi.org/10.1088/0031-9155/40/5/007>
- Matysiak, W., Prestwich, W. V., and Byun, S. H. "Precise measurements of the thick target neutron yields of the  ${}^7\text{Li}(p,n)$  reaction." *Nuclear Instruments and Methods in Physics Research, Section A: Accelerators, Spectrometers, Detectors and Associated Equipment*, Vol. 643, No. 1, (2011), 47–52. <https://doi.org/10.1016/j.nima.2011.04.034>
- Mildner, D. F. R., and Lamaze, G. P. "Neutron Transmission of Single-Crystal Sapphire." *Journal of Applied Crystallography*, Vol. 31, No. 6, (1998), 835–840. <https://doi.org/10.1107/S0021889898005846>

## Persian Abstract

### چکیده

در این کار مقایسه شش پرتوی نوترونی با استفاده از کد MCNPX مونت کارلو با هدف رادیوگرافی نوترونی حرارتی انجام شده است. نوترون‌های لازم از طریق واکنش  ${}^7\text{Li}(p,n)$  برای پرتو پروتون ۱ میلی‌آمپر با انرژی ۲/۳، ۲/۵، ۳، ۴، ۵/۱ و ۵ MeV تولید شده‌اند. طراحی امکانات برای دستیابی به حداکثر شار نوترون حرارتی در موقعیت هدف مورد بررسی انجام شد. تعداد زیادی از شبیه‌سازی‌ها برای هر منبع تحت شرایط مختلف انجام شد. انرژی بالاتر پرتو پروتون شدت بیشتری برای منبع نوترون فراهم می‌کند اما در عین حال طیف تولید شده به ناحیه نوترون سریع منتقل می‌شود. پروتون‌هایی با انرژی از ۲/۳ تا ۳ MeV مناسب‌ترند. وقتی محتوای نوترون حرارتی مسئله اصلی طراحی تسهیلات است. نوترون‌های تولید شده توسط پرتو پروتون در گستره انرژی ۵/۴ مگا الکترون ولت شار نوترون حرارتی بالاتری را با هزینه محتوای نوترون حرارتی فراهم می‌کنند. انتخاب نهایی یک سازش بین محتوای نوترون حرارتی که قابل تحمل است، در ترکیب با یک شار نوترون حرارتی قابل استفاده می‌باشد.